Applied Energy 220 (2018) 480–495

Contents lists available at ScienceDirect

Applied Energy

journal homepage: www.elsevier.com/locate/apenergy

A novel hybrid method of forecasting crude oil prices using complex network science and artificial intelligence algorithms

Minggang Wang[a,b,c], Longfeng Zhao[c], Ruijin Du[c,d], Chao Wang[c,e], Lin Chen[c,f], Lixin Tian[a,d,*], H. Eugene Stanley[c]

[a] School of Mathematical Science, Nanjing Normal University, Nanjing 210042, Jiangsu, China
[b] Department of Mathematics, Nanjing Normal University Taizhou College, Taizhou 225300, Jiangsu, China
[c] Center for Polymer Studies and Department of Physics, Boston University, Boston, MA 02215, USA
[d] Energy Development and Environmental Protection Strategy Research Center, Jiangsu University, Zhenjiang 212013, Jiangsu, China
[e] College of Economics and Management, Beijing University of Technology, Beijing 100124, China
[f] School of Management, Northwestern Polytechnical University, Xi'an 710072, Shanxi, China

HIGHLIGHTS

- A novel prediction paradigm (DFN-AI) is proposed based on complex network and AI algorithms.
- DFN analysis technique is performed to extract the fluctuation features in original data.
- A new data reconstruction method is designed by using the extracted data.
- A certain artificial intelligence tool is employed to model the reconstructed data.
- Empirical results demonstrate the effectiveness and robustness of DFN-AI method.

ARTICLE INFO

Keywords:
Complex network
Artificial intelligence algorithms
Crude oil price prediction

ABSTRACT

Forecasting the price of crude oil is a challenging task. To improve this forecasting, this paper proposes a novel hybrid method that uses an integrated data fluctuation network (DFN) and several artificial intelligence (AI) algorithms, named DFN-AI model. In the proposed DFN-AI model, a complex network time series analysis technique is performed as a preprocessor for the original data to extract the fluctuation features and reconstruct the original data, and then an artificial intelligence tool, e.g., BPNN, RBFNN or ELM, is employed to model the reconstructed data and predict the future data. To verify these results we examine the daily, weekly, and monthly price data from the crude oil trading hub in Cushing, Oklahoma. Empirical results demonstrate that the proposed DFN-AI models (i.e., DFN-BP, DFN-RBF, and DFN-ELM) perform significantly better than their corresponding single AI models in both the direction and level of prediction. This confirms the effectiveness of our proposed modeling of the nonlinear patterns hidden in crude oil prices. In addition, our proposed DFN-AI methods are robust and reliable and are unaffected by random sample selection, sample frequency, or breaks in sample structure.

1. Introduction

Because crude oil is a basic energy source and its price volatilities strongly impact a country's economic development, social stability, and national security [1], accurately predicting crude oil price fluctuations is a consistently active topic of research. The research on crude oil price fluctuations being carried out internationally is made more complex by the interplay among many factors—including market supply and demand [2], the US dollar exchange rate [3], speculative trading [4], geopolitical conflicts [5], and natural disasters [6]—that introduces a high level of noise into the crude oil data. Thus the crude oil prices, which exhibit such complex volatility characteristics as nonlinearity and uncertainty, are difficult to forecast and any results obtained uncertain. Therefore, crude price prediction remains a huge challenge.

Up to now, there has been a raft of literature discussing crude oil price forecasting. Among these prediction models, one of the most

* Corresponding author at: School of Mathematical Science, Nanjing Normal University, Nanjing 210042, Jiangsu, China.
E-mail addresses: magic821204@sina.com (M. Wang), zlfccnu@mails.edu.cn (L. Zhao), dudo999@126.com (R. Du), chaowanghn@vip.163.com (C. Wang), clnwpu@126.com (L. Chen), tianlx@ujs.edu.cn (L. Tian), hes@bu.edu (H. Eugene Stanley).

https://doi.org/10.1016/j.apenergy.2018.03.148
Received 4 January 2018; Received in revised form 5 March 2018; Accepted 28 March 2018
Available online 30 March 2018
0306-2619/

Nomenclature

X	original time series
N	data size
P	fluctuation series of X
S	symbol series
k	number of the symbols
s_i	symbol
L	length of the sliding window
l	sliding step
r	threshold
FM_i	the ith fluctuation modes
$\widehat{M}$	number of the fluctuation modes
M	number of different fluctuation modes
v_i^t	node numbered i at time t
$V_{i\to j}^{t+1}$	set of all out-neighbor nodes of v_i^t
W	weight
η	learning rate
E	the gradient of error function
B_i	the prototype of the input vectors
σ_i	the width of RBF unit i
$\widehat{X}$	predicted data
$f(x)$	the activation function
b_i	the bias of hidden node i
β_i	the weights of hidden neuron i to output neurons
EX	extracted data
SX	sub data of original data
α	the selectivity coefficient
RX	the reconstructed data

Abbreviations

DFN	data fluctuation network
BPNN	back propagation neural network
RBFNN	radial basis function neural network
ELM	extreme learning machine
DFN-BP	hybrid model based on DFN and BPNN
DFN-RBF	hybrid model based on DFN and RBFNN
DFN-ELM	hybrid model based on DFN and ELM
MAPE	mean absolute percentage error
RMSE	root mean square error
Dstat	directional statistic
DMS	Diebold-Mariano statistic

important models is econometric model. For instance, Lanza et al. [7] used cointegration and error correction models (ECM) to predict crude oil prices from January 2002 to June 2002. Murat et al. [8] proposed a vector error correction model (VECM) to forecast oil price movements and crack spread futures. Baumeister et al. [9] used vector autoregressive (VAR) to forecast WTI spot price. Xiang et al. [10] used an autoregressive integrated moving average (ARIMA) model to predict the Brent crude oil. Sadorsky [11] used several GARCH models to forecast the daily volatility in petroleum futures price returns. Fan et al. [12] introduced GARCH type models based on generalized error distribution (GED) to examine the risk spillover effect between West Texas Intermediate (WTI) and Brent crude oil markets. Kang et al. [13] then proposed a variety of conditional volatility models, including GARCH, IGARCH, CGARCH, and FIGARCH, to forecast the volatility of crude oil markets, and found that the CGARCH and FIGARCH models can forecast volatility persistence. Mohammadi et al. [14] investigated the out-of-sample forecasting performance of four volatility models—GARCH, EGARCH, APARCH and FIGARCH over January 2009 to October 2009. Hou and Suardi [15] focused on two crude oil markets, Brent and WTI, considered an alternative approach involving nonparametric method to model and forecast oil price return volatility. The main results of the above mentioned econometric models are listed in Table 1 (the upper part). In essence there are two different types of econometric models. The first is a structural model of the price of oil, including ECM [7], VECM [8], VAR [9] et al., depending on fundamental data such as demand and supply and is implemented through the use of a linear regression. This structural modeling approach includes explanatory variables other than just the past data of oil prices into the process. The second is a time series approach, including ARIMA [10], GARCH-type models [11–15] et al., only looking at the history of price to determine future price movement. Because they are able to capture time-varying volatility, econometric models have improved the accuracy of forecasting, but because they assume the data to be stationary, regular, and linear they cannot accurately model time series that are complex, irregular, and nonlinear [7–15].

In addition to the classic econometric approaches, artificial intelligence (AI) methods have been used to uncover the inner complexity of oil prices. For example, Moshiri et al. [16] set up a nonlinear and flexible artificial neural network (ANN) model to forecast daily crude oil futures prices traded at the New York Mercantile Exchange (NYMEX). Kaboudan [17] evaluated forecasts produced by two competing compumetric forecasting methods: genetic programming (GP) and artificial neural networks (ANN). Mostafa et al. [18] forecasted oil prices using gene expression programming (GEP) and artificial neural network (ANN) models. Kaboli et al. [19,20] developed artificial cooperative search algorithm (ACSA) and GEP to provide better-fit solution and improve the accuracy of estimation. Xie et al. [21] proposed a support vector machine (SVM) to forecast crude oil prices and compared its performance with ARIMA and back propagation neural network (BPNN). Shin et al. [22] employed semi-supervised learning (SSL) to forecast the upward and downward movement of oil prices. Yusof et al. [23] proposed least squares support vector machine (LSSVM) method of the oil futures price forecasting. Zhao et al. [24] introduced deep learning approach (SDAE) for WTI crude oil spot price forecasting. The main results of the above mentioned AI models are listed in Table 1 (the middle part). Unlike econometric models [7–15], artificial intelligence methods are able to model such complex characteristics as nonlinearity and volatility. Artificial intelligence methods also have disadvantages, For example, ANN and BPNN often suffer from local minima and over-fitting, while other AI models, such as SVM and GP including ANN, are sensitive to parameter selection [16–24].

Because single prediction models—including both econometric models and AI methods—are limited, many studies are now using hybrid methods to forecast crude oil prices. Some typical literature regarding the hybrid methods for crude oil price forecasting can be found in Table 1 (the bottom part). Overall, the hybrid methods often imply the combination of interdisciplinary methods to use their strengths and can be roughly classified into two categories: (1) the combination among AI models, such as the empirical mode decomposition (EMD) based neural network ensemble learning paradigm [25], the hybrid model combining the dynamic properties of multilayer back propagation neural network and the recent Harr A trous wavelet decomposition, i.e., HTW-MPNN [26], the hybrid model built upon EMD based on the feed-forward neural network (FNN) modeling framework incorporating the slope based method (SBM), i.e., EMD-SBM-FNN [27], a decomposition-and-ensemble learning paradigm integrating ensemble empirical mode decomposition (EEMD) and extended extreme learning machine (EELM), i.e., EEMD-EELM [28], the compressed sensing based learning paradigm, integrating compressed sensing based de-noising (CSD) and certain artificial intelligence (AI), i.e., CSD-AI [29], the alternative approach based on a genetic algorithm and neural network (GA-NN) [30], the hybrid AI system framework integrating web-based

Table 1
Summary of studies on crude oil price forecasting via various methods.

Types	Typical literature	Forecasting models	Forecasting period	Data type	Main results
Econometric models	Lanza et al. [7]	ECM	2002/01–2002/06	Daily	The cointegration marginally improves static forecasts
	Murat et al. [8]	VECM	2000/01–2008/02	Weekly	VECM outperforms the random walk model (RWM)
	Baumeister et al. [9]	VAR	1991/01–2010/12	Monthly	VAR tend to have lower MSPE at short horizons than AR and ARMA
	Xiang [10]	ARIMA	2012/11–2013/04	Daily	ARIMA possess good prediction effect and can be used as short-term prediction
	Sadorsky [11]	GARCH type models	1988/02–2003/01	Daily	TGARCH model fits well for heating oil and natural gas and the GARCH model fits well for crude oil and unleaded gasoline
	Fan et al. [12]	GED-GARCH	1987/05–2006/08	Daily	GED-GARCH model has superior power in the out-of-sample forecast compared with the popular HSAF method
	Kang et al. [13]	CGARCH and FIGARCH models	1992/01–2006/12	Daily	CGARCH and FIGARCH models provide superior performance in out-of-sample volatility forecasts GARCH and IGARCH models
	Mohammadi et al. [14]	GARCH, EGARCH, APARCH,FIGARCH	2009/01–2009/10	Weekly	APARCH model outperforms the others.
	Hou et al. [15]	Nonparametric GARCH model	1992/01–2010/07	Daily	The non-parametric GARCH model has a better forecast than the traditional GARCH model
AI models	Moshiri et al. [16]	ANN	1983/04–2003/01	Daily	ANN model outperforms ARMA and GARCH models
	Kaboudan [17]	GP	1993/01–1998/12	Monthly	GP has advantage over random walk predictions while the ANN forecast proved inferior
	Mostafa et al.[18]	GEP	1986/01–2012/06	Daily	GEP model outperforms the ANN and ARIMA models
	Xie et al. [21]	SVM	1970/01–2003/12	Monthly	SVM outperforms ARIMA and BPNN
	Shin et al. [22]	SSL	1992/01–2008/06	Monthly	SSL outperforms ANN and SVM
	Yusof et al. [23]	LSSVM	2006/01–2012/06	Daily	LSSVM forecasting model outperforms SVM and RBF network model
	Zhao et al. [24]	SDAE	1986/01–2016/05	Monthly	SDAE has superior power compared with traditional machine learning models
Hybrid models	Yu et al. [25]	EMD based neural network ensemble learning paradigm	1986/01–2006/09	Daily	EMD-based neural network ensemble learning paradigm performs better than traditional AI models
	Jammazi et al.[26]	HTW-MBPNN	1988/01–2010/03	Monthly	HTW-MBPNN perform better than the conventional BPNN
	Xiong et al. [27]	EMD-SBM-FNN	2000/01–2011/12	Weekly	EMD-SBM-FNN using the MIMO strategy is a very promising prediction technique with high-quality forecasts and accredited computational loads for multi-step-ahead crude oil price forecasting
	Yu, Dai et al. [28]	EEMD-EELM	1986/01–2013/10	Daily	EEMD-EELM is significantly superior to single EELM
	Yu, Zhao et al. [29]	CSD-AI	2011/01–2013/07	Daily	CSD-AI models outperform their single benchmarks in both level and directional predictions
	Chiroma et al. [30]	GA-NN	2008/05–2011/12	Monthly	The GA-NN approach is able to improve prediction accuracy, and to simplify the complexity of the NN model structure
	Wang et al. [31]	A hybrid AI system framework	2000/01–2002/12	monthly	The proposed approach is significantly effective and practically feasible
	Zhang et al. [1]	EEMD-LSSVM-PSO-GARCH	2013/01–2013/12; 2000/01–2008/07; 1990/01–2013/07	Daily; weekly; monthly	The newly proposed hybrid method has a strong forecasting capability for crude oil prices

text mining and rule-based expert system with ANN-based time series forecasting techniques [31]. (2) The combination of AI methods and econometric methods, such as a hybrid method that combines EEMD, least square support vector machine particle swarm optimization (LSSVM-PSO), and the GARCH model, i.e., EEMD-LSSVM-PSO-GARCH [1]. Empirical analysis results repeatedly demonstrate that hybrid forecast methods are more accurate than single methods (see Table 1). This is the case because hybrid methods combine single models such that the merits of each offset the defects of others. At the same time, the calculation process required in hybrid methods is complicated. In other words, the hybrid forecasting models are more likely to be advocated in recent literature, which also gives some hints for our research in this paper.

As mentioned above, the most important challenge in modeling crude oil price is the complexity in terms of interactive inner factors, which leads to a high level of noise corrupting the original data and thus largely weakening the prediction capability of models. Actually, noise reduction techniques already being employed include entropy-based wavelet de-noising [32], hybrid slantlet de-noising based on the least squares support vector regression model [33], exponential smoothing based on neural networks [34], and the extended Kalman filter method [35]. However, all of these techniques have a fatal weakness: their fixed basis design makes them sensitive to parameter settings. In recent years complex network theory has been widely used to analyze nonlinear time series. Complex network theory uses algorithms to transform a nonlinear time series into corresponding complex networks and uses the typology of complex networks to draw out regular fluctuation patterns. The application of complex network theory has been widely effective in determining the essential characteristics of a time series. It has produced a number of new algorithms that can transform a time series into a complex network system. Among them are the visibility graph (VG) [36], the pseudo-periodic time series transform algorithm [37], phase space reconstruction [38], and the coarse graining of phase space [39]. A large number of researchers have recently applied complex network theory to the study of energy price fluctuations and have produced many valuable results [40–51]. In other words, the rapid development of complex network time series analysis technology provides a new perspective for eliminating the noise in the original data.

Therefore, due to the complexity in terms of high level of noise in crude oil price data, this paper focus on the following questions: How to eliminate the noise from original data using the complex network time series analysis techniques? How to determine regular fluctuation patterns and extract the nonlinear patterns hidden in original data efficiently? How to enhance the robustness of analysis and forecasting performance for crude oil price? To date there have fewer related studies. To address the above questions, here we combine complex network analysis and AI predictive methods to formulate a novel hybrid prediction model for crude oil price fluctuations. Different from the previous studies and four main novel contributions in our studies are as follows: (1) a complex network analysis of the original data is first performed to extract the fluctuation features using the topological structure of the network. (2) A new data reconstruction method is designed by using the extracted fluctuation features data and the original data. (3) A certain AI tool, e.g., BPNN, RBFNN, or ELM, is employed to model the reconstructed data and generate the final prediction. (4) Empirical results demonstrate that the proposed data fluctuation network (DFN) AI models (i.e., DFN-BP, DFN-RBF, and DFN-ELM) perform significantly better than their corresponding single AI models in both the direction and level of prediction. And our proposed DFN-AI methods are robust and reliable and are unaffected by random sample selection, sample frequency, or breaks in sample structure.

We organize the rest of this paper as follows. Section 2 provides a detailed description of how the proposed model was formulated. Section 3 presents a sensitivity analysis of the parameters. Section 4 describes and discusses the crude oil forecasting results. At the end of the paper we present our conclusions and propose possible future lines of research.

2. Methodology

2.1. Complex network analysis of time series

Complex network theory has been recently applied to the analysis of time series and has yielded high-quality results [36–39]. There are two steps in this approach. The first uses algorithms to map the time series into a complex network. The second uses the topological structure of the network to uncover the essential characteristics of the time series.

2.1.1. Map the time series into a data fluctuation network (DFN)

Here we use coarse geometry theory to map the time series into a directed and weighted network [39,43]. In the calculation process we denote the time series $X = \{X(t)\}$, with $t = 1,2,...,N$, and the fluctuation series $P = \{P(t)\}$, which we obtained using

$$P(t) = \frac{X(t)-X(t-1)}{X(t-1)}, \tag{1}$$

where $X(0) = X(1)$ and $P(1) = 0$. We next define k symbols $\{s_1,s_2,...,s_k\}$, which denote the fluctuation state of the time series at time t. To preserve the symmetries of symbols, k satisfies two conditions: it is an odd number and $k \geqslant 3$. We then set $k-2$ thresholds $\{r_{k-3/2},r_{k-5/2},...,r_0,...,-r_{k-5/2},-r_{k-3/2}\}$, where $r_0 = 0$. Using these thresholds, we map the fluctuation series $\{P(t)\}$ into a continuous symbol series $S = \{S(t)\}$ and $S(t) \in \{s_1,s_2,...,s_k\}$. For example, when $k = 5$ we have

$$S(t) = \begin{cases} s_1, P(t) > r_1, \\ s_2, 0 < P(t) \leqslant r_1, \\ s_3, P(t) = r_0 = 0, \\ s_4, -r_1 \leqslant P(t) < 0, \\ s_5, P(t) < r_1, \end{cases} \qquad r_1 = \frac{1}{N}\sum |P(t)| \tag{2}$$

Note that we can either increase or decrease the number of symbols in different time series according to what the problem requires. The sliding window method [31] then used to divide the continuous symbol sequence $\{S(t)\}$ into modes. Here there are $\widehat{M} = [(N-L)/l + 1]$ fluctuation modes, where L is the sliding window length and l the sliding step. The different fluctuation modes are denoted to be FM_i, $i = 1,2,...,M$, $M \leqslant \widehat{M}$ where each fluctuation mode is a network node and transformations among modes are the edges between nodes. The fluctuating modes evolve into each other with time, and the weight of an edge is defined to be the transformation frequency. Thus, the directed and weighted data fluctuation network is constructed and denoted to be $DFN(r,k,L,l)$. In summary, we use five characters $\{s_1,s_2,s_3,s_4,s_5\}$ to represent the fluctuation sequence, let $L = 5$, and $l = 1$, then the mapping process of $DFN(r,k,L,l)$ is shown in Fig. 1.

2.1.2. Extract the fluctuation features accordingly to the topological structure of the DFN

Using the topological structure of the DFN, the fluctuation characteristics of time series can be characterized. For example, let $k = 5$, $L = 5$, $l = 1$ and denote the node at time t to be v_i^t, where $t = 1,2,...,\widehat{M}$, $\widehat{M} = N-L+1$, and $i = 1,2,...,M$. Since the DFN is a directed network, with the exception of the first and the last nodes every node has an in-neighbor node and out-neighbor node. Using the construction method of the DFN (see Section 2.1.1), we see two types of connection between node $v_i^{\widehat{M}}$ and its out-neighbor nodes:

(i) When $v_i^{\widehat{M}}$ has no out-neighbor node. If the mapped symbol series of the time series is $\{S(t')\}_{t'=1,2,...,10} = \{s_3s_4s_4s_1s_2s_1s_5s_5s_1s_2\}$, then the nodes of the DFN are $v_1^1 = s_3s_4s_4s_1s_2$, $v_2^2 = s_4s_4s_1s_2s_1$, $v_3^3 = s_4s_1s_2s_1s_5$,

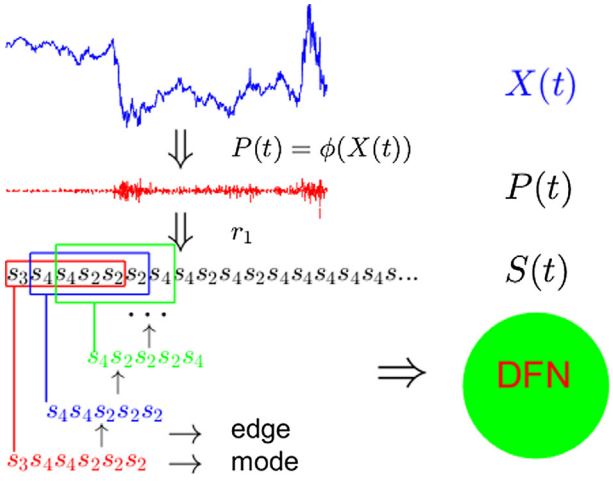

Fig. 1. The mapping process of *DFN* (*r*,*k*,*L*,*l*).

Fig. 2(b) shows the network structure. Here node v_2^{10} (shown in green) has two out-neighbor nodes. We can also find that each node here has an out-neighbor node.

Fig. 2(b) shows the network structure of the DFN when the size of the sample data is sufficiently large. Fig. 2(a) shows a network structure of the DFN that requires an adjustment of the parameters. There are two ways of adjusting this structure so that it conforms to that in Fig. 2(b). (i) Reduce the number of symbols in the coarse graining process and adopt three characters, i.e., $k = 3$, when coarse graining the fluctuation series. (ii) Reduce the number characters during the construction of the fluctuation mode, e.g., adopting a three-character combination (i.e., $L = 3$). Using these two methods a small sample dataset can be converted into a usable DFN. The sensitivity analysis parameters of the DFN is described in Section 3.After building the DFN we select the target node based on the input data. Using the above analysis, the target node must have an out-neighbor node, e.g., in Fig. 2(b) the green node is the target node and nodes v_3^3 and v_5^6 are its out-neighbor nodes. The set of all out-neighbor nodes of target v_i^t is

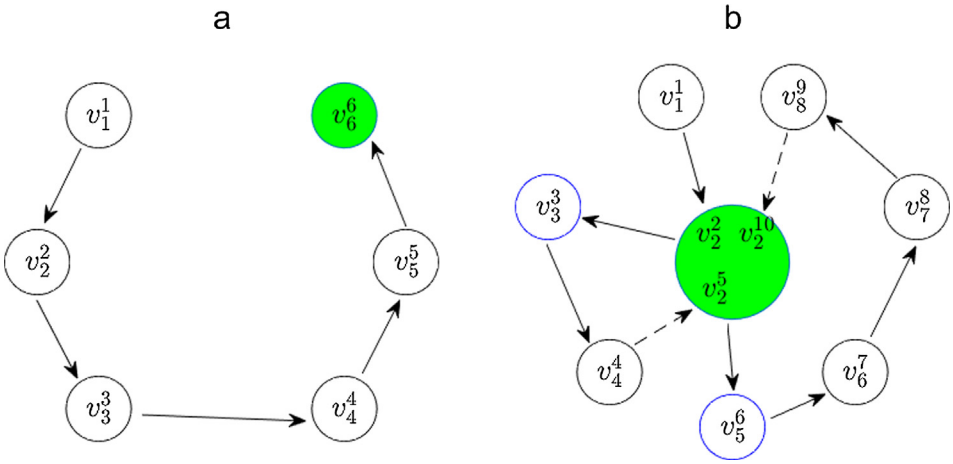

Fig. 2. Two different types of DFN.

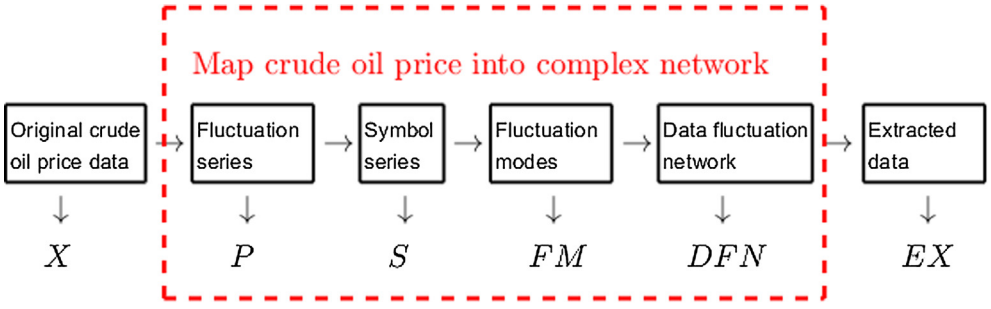

Fig. 3. The process of the complex network analysis of crude oil price.

$v_4^4 = s_1s_2s_1s_5s_5$, $v_5^5 = s_2s_1s_5s_5s_1$ and $v_6^6 = s_1s_5s_5s_1s_2$. Fig. 2(a) shows the network structure. Here node v_6^6 (shown in green[1]) has no out-neighbor node.

(ii) When $v_i^{\widehat{M}}$ has out-neighbor nodes. If the mapped symbol series of the time series is

$$\{S(t')\}_{t'=1,2,\ldots,14} = \{s_4s_4s_1s_2s_4s_1s_2s_4s_1s_4s_1s_2s_4s_1\},$$

then the nodes of the DFN are $v_1^1 = s_4s_4s_1s_2s_4$, $v_2^2 = s_4s_1s_2s_4s_1$, $v_3^3 = s_1s_2s_4s_1s_2$, $v_4^4 = s_2s_4s_1s_2s_4$, $v_2^5 = s_4s_1s_2s_4s_1$, $v_5^6 = s_1s_2s_4s_1s_4$, $v_6^7 = s_2s_4s_1s_4s_1$, $v_7^8 = s_4s_1s_4s_1s_2$, $v_8^9 = s_1s_4s_1s_2s_4$ and $v_2^{10} = s_4s_1s_2s_4s_1$.

[1] For interpretation of color in Fig. 2, the reader is referred to the web version of this article.

$$V_{i\to j}^{t+1} = \{v_{i\to j}^t\}_{j\in[1,M],t\in[1,\widehat{M}]} \tag{3}$$

The parameters of DFN are usable when the node that appears at time $t + 1$ is an element in the set $V_{i\to j}^{t+1}$. Thus there are two ways of extracting the future fluctuation features of the target node, (i) using all the elements in set $V_{i\to j}^{t+1}$ or (ii) using the element with the greatest strength in set $V_{i\to j}^{t+1}$. Fig. 3 shows a summary of the complex network analysis of a crude oil price series.

2.2. Artificial intelligence algorithms

A series of artificial intelligence algorithms for forecasting crude oil prices were recently developed, and they have proven to be superior to

traditional forecasting models [16–24]. Here we focus on three, (i) the back propagation neural network (BPNN), (ii) the radial basis function neural network (RBFNN), (iii) and the extreme learning machine (ELM) [52–55].

2.2.1. Back propagation neural network (BPNN)

The back propagation neural network (BPNN) model is one of the most widely used artificial intelligence algorithms for classification and prediction [52]. This technique is an advanced multiple regression analysis that deals with responses that are more complex and non-linear than those of standard regression analysis. The basic formula of the BP algorithm is

$$W(n) = W(n-1) - \Delta W(n), \tag{4}$$

where

$$\Delta W(n) = \eta \frac{\partial E}{\partial W}(n-1) + \gamma \Delta W(n-1), \tag{5}$$

where W is the weight, η is the learning rate, E is the gradient of error function, and $\gamma \Delta W(n-1)$ is the incremental weight. Because the BPNN uses the gradient method the learning convergent velocity is slow and a convergence to the local minimum always occurs. In addition, the selection of the learning and inertial factors affects the convergence of the BPNN, which is determined by the level of experience. Thus the usefulness of the BPNN is limited.

2.2.2. Radial basis function neural network (RBFNN)

The radial basis function (RBF) neural network has been widely applied in the neural network community [53]. The RBFNN is a mapping, i.e., $\Re^r \to \Re^s$. When $X \in \Re^r$ is the input vector and $B_i \in \Re^r$, $(1 \leqslant i \leqslant u)$ the prototype of the input vectors, the output of each RBF unit is

$$R_i(X) = R_i(\|X - B_i\|), \quad i = 1,2,...,u, \tag{6}$$

where $\|\cdot\|$ is the Euclidean norm on the input space. Because it can be factored, the Gaussian function is the preferred radial basis function. Thus

$$R_i(X) = \exp\left[-\frac{\|X - B_i\|^2}{\sigma_i^2}\right], \tag{7}$$

where σ_i is the width of RBF unit i. The output $Y_j(X)$ unit j of an RBFNN is

$$Y_j(X) = \sum_{i=1}^{u} R_i(X) \times W(j,i), \tag{8}$$

where $R_0 = 1$, $W(j,i)$ is the weight or strength of receptive field i to the output j, and $W(j,0)$ is the bias of output j. Geometrically, an RBFNN partitions the input space into several hyper sphere subspaces. This introduces several challenges into the development of the RBF algorithm, e.g., over-fitting, overtraining, the small-sample effect, and the singular problem.

2.2.3. Extreme learning machine (ELM)

The extreme learning machine (ELM) was originally applied to single hidden-layer feed-forward neural networks and then extended to generalized feed-forward networks [54,55]. For a set of training samples $\{(X_j,C_j)\}_{j=1}^{N}$ with N samples and C classes, the single hidden layer feed-forward neural network with h hidden nodes and activation function $f(x)$ is

$$\sum_{i=1}^{h} \beta_i f_i(X_j) = \sum_{i=1}^{h} \beta_i f(W_i \cdot X_j + b_i) = Y_j, \quad j = 1,2,...,N, \tag{9}$$

where $X_j = [x_{j1},x_{j2},...,x_{jn}]^T$, $C_j = [c_{j1},c_{j2},...,c_{jm}]^T$, $W_i = [w_{i1},w_{i2},...,w_{in}]^T$, and b_i are the input, its corresponding output, the connecting weights of hidden neuron i to input neurons, and the bias of hidden node i, respectively, and $\beta_i = [\beta_{i1},\beta_{i2},...,\beta_{im}]^T$ are the connecting weights of hidden neuron i to output neurons, and Y_j the actual network output with respect to input X_j. Because the hidden parameters $\{W_i,b_i\}$ can be randomly generated during the training period without tuning, ELM solves a compact model that minimizes the error between C_j and Y_j, i.e.,

$$\min_{\beta} \|H\beta - C\|_F, \tag{10}$$

with

$$H(W_1,W_2,...,W_h,b_1,b_2,...,b_h) = \begin{bmatrix} f(W_1 \cdot X_1 + b_1) & \cdots & f(W_h \cdot X_1 + b_h) \\ \vdots & \cdots & \vdots \\ f(W_1 \cdot X_N + b_1) & \cdots & f(W_h \cdot X_N + b_h) \end{bmatrix}, \beta = \begin{bmatrix} \beta_1^T \\ \vdots \\ \beta_h^T \end{bmatrix}, C = \begin{bmatrix} c_1^T \\ \vdots \\ c_N^T \end{bmatrix}. \tag{11}$$

Here H is the hidden layer output matrix and β the output weight matrix. Eq. (10) is a least squares problem with a solution $\widehat{\beta} = H^{-1}C$, where H^{-1} is the pseudo-inverse of H. The merit of ELM is that only the output weights are needed when randomly selecting the hidden node parameters (input weights and bias). Its weakness is that it cannot effectively handle noisy time series.

2.3. The novel hybrid method for crude oil price forecast

Using these techniques, a novel hybrid DFN-AI learning paradigm is formulated for crude oil prices (see Fig. 4). There are three steps in the proposed DFN-AI learning paradigm, i.e., extract the fluctuation features, reconstruct the data, and formulate the forecast.

STEP 1: Construct the data fluctuation network (DFN) and extract the fluctuation features.

The original data is first mapped on a directed and weighted data fluctuation network (DFN) using the complex network analysis of the time series shown in Figs. 1 and 4. We then use the topological structure of the DFN to extract the fluctuation features of the crude oil prices. For example, if the original data $X = \{X(t)\}$, with $t = 1,2,...,N$, assume that the length of sliding window is L, the sliding step is l, then the original data X can be rewritten

$$X = \begin{bmatrix} X(1) & X(2) & \cdots & X(\widehat{M}) \\ \vdots & \vdots & \cdots & \vdots \\ X(L) & X(L+1) & \cdots & X(L+\widehat{M}-1) \end{bmatrix} = [X_1 X_2 \cdots X_{\widehat{M}}]. \tag{12}$$

where $X_i = [X(i),...,X(i+L-1)]^T$, $i = 1,2,...,\widehat{M}$, $\widehat{M} = (N-L)/l-1$, then using the method of Section 2.1.2, the extracted fluctuation data features are

$$EX = \begin{bmatrix} EX(1) & EX(2) & \cdots & EX(D) \\ \vdots & \vdots & \cdots & \vdots \\ EX(L) & EX(L+1) & \cdots & EX(L+D-1) \end{bmatrix} = [X_{i1} X_{i2} \cdots X_{iD}]. \tag{13}$$

where $D < \widehat{M}$, $ij \in [1,\widehat{M}]$, $j = 1,2,\cdots,D$.

STEP 2: Reconstruct data

We introduce the sub data of original data, $SX = \{X(t')\}$, with $t' = N - [\alpha N] + 1,\cdots,N$, $\alpha \in (0,1]$, where $[x]$ is integer-valued function, α is the selectivity coefficient, when $\alpha = 1$, then $SX = X$. Using the sub data SX and the extracted fluctuation features data EX, the new data RX is obtained for further analysis, i.e.,

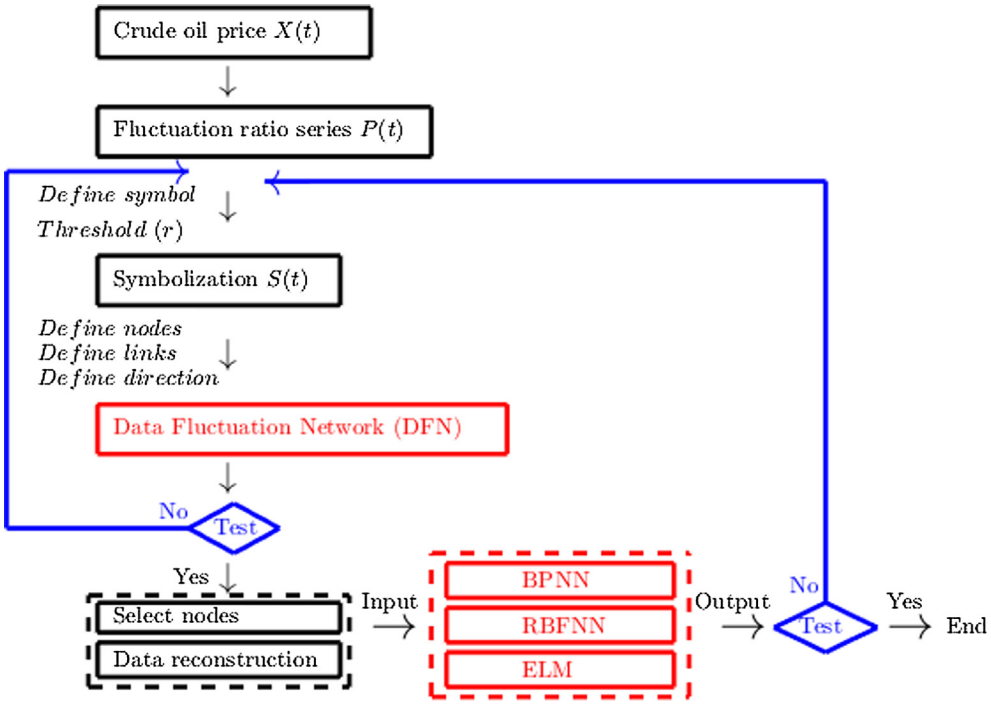

Fig. 4. The procedures of DFN-AI algorithm for crude oil price forecasting.

$$RX = \begin{bmatrix} EX(1) & EX(2) & \cdots & EX(D) & SX(1) & \cdots & SX([\alpha N]-L+1) \\ \vdots & \vdots & \cdots & \vdots & \vdots & \cdots & \vdots \\ EX(L) & EX(L+1) & \cdots & EX(L+D-1) & SX(L) & \cdots & SX([\alpha N]) \end{bmatrix} \tag{14}$$

or

$$RX = \begin{bmatrix} EX(1) & EX(2) & \cdots & EX(D) & X(N-[\alpha N]+1) & \cdots & X(\widehat{M}) \\ \vdots & \vdots & \cdots & \vdots & \vdots & \cdots & \vdots \\ EX(L) & EX(L+1) & \cdots & EX(L+D-1) & X(N-[\alpha N]+L) & \cdots & X(L-\widehat{M}-1) \end{bmatrix}. \tag{15}$$

STEP 3: Forecasting using artificial intelligence algorithms

After data reconstruction, we use AI techniques BPNN, RBFNN, or ELM to model the reconstruction data RX, then a novel hybrid DFN-AI learning paradigm for crude oil price can be formulated, as illustrated in Fig. 5. Combining the data fluctuation network analysis technology and BPNN, RBFNN, or ELM, the hybrid prediction model DFN-BP, DFN-RBF and DFN-ELM can be built, respectively.

2.4. Performance evaluation criteria

To measure the forecasting accuracy of these proposed methods, we apply the widely-used mean absolute percentage error (MAPE) and root mean square error (RMSE) [1,17,23,46] methods, defined as

$$MAPE = \frac{1}{N}\sum_{t=1}^{N}\left|\frac{X(t)-\widehat{X}(t)}{X(t)}\right|. \tag{16}$$

and

$$RMSE = \sqrt{\frac{\sum_{t=1}^{N}(\widehat{X}(t)-X(t))^2}{N}}. \tag{17}$$

where $\widehat{X}(t)$ and $X(t)$ are the predicted and real values at time t, respectively, and N is the size of the dataset being tested. The MAPE technique measures the mean absolute relative error of the prediction models, and the RMSE technique measures their standard deviation. In using these error criteria we find that the smaller the MAPE and RMSE values the greater the level of model accuracy. Our most important concern, however, is the *directional tendency* of data fluctuations—-whether they are upward, stable or downward—and we measure them using

$$Dstat = \frac{1}{N}\sum_{t=1}^{N} a(t), \quad a(t) = \begin{cases} 1, & (X(t+1)-X(t))(\widehat{X}(t+1)-X(t)) \geqslant 0 \\ 0, & otherwise \end{cases}. \tag{18}$$

The closer the Dstat value is to 1, the higher the accuracy of the directional prediction of the models, and the closer the Dstat value is to 0, the lower the accuracy of their directional predictions.

The Diebold-Mariano (DM) statistic [24,56] is used to measure the differences in the predictive accuracies of the forecasting models. Here the loss function is set to the mean square prediction error (MSPE). The null hypothesis is that the MSPE value of the tested model is not lower than that of the benchmark model. The DM statistic is defined

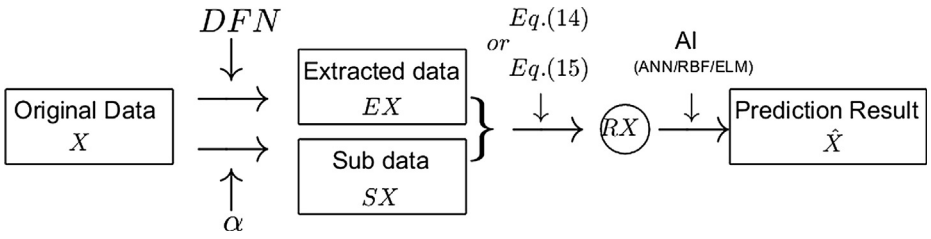

Fig. 5. The overall process of DFN-AI learning paradigm.

$$DMS = \frac{\overline{D}}{\sqrt{V_{\overline{D}}/M}}, \tag{19}$$

where $\overline{D} = \frac{1}{M}\sum_{t=1}^{M} d(t)$, $d(t) = (X(t)-\widehat{X}_{test}(t))^2-(X(t)-\widehat{X}_{bench}(t))^2$, $V_{\overline{D}} = \gamma_0 + 2\sum_{q=1}^{\infty}\gamma_q$, $\gamma_q = \mathrm{cov}(d_t,d_{t-q})$. $\widehat{X}_{test}(t)$ and $\widehat{X}_{bench}(t)$ are the predicted values for $X(t)$ calculated by the tested model and its benchmark model, respectively, at time t.

3. Sensitivity analysis of the parameters in data fluctuation network

The DFN (r, k, L, l) is constructed by mapping the time series on the directed and weighted network. The associated network then inherits some of the time series structure. We examine, without loss of generality, how the associated directed and weighted network inherits information from the time series. We test four time series of 1000 data each, including a chaotic time series generated from a logistic map ($\mu = 4$), a chaotic time series generated from a Lorenz system ($a = 10$, $b = 28$, $c = 8$), an independent and identically distributed (*i.i.d.*) random series from a uniform distribution $f(x) = U[0,1]$, and the crude oil price series from 4 April 1983 to 30 March 1987. Three of these time series are dynamic systems and the fourth is a real price series. Thus their inner characteristics differ. The parameters are set at $k = 5$, $L = 5$, $l = 1$, and r_1 calculate

$$r_1 = \frac{1}{N}\sum_{t=1}^{N} |P(t)|. \tag{20}$$

Fig. 6 shows the network structure of DFNs mapped from the four time series types. Note that their structures (e.g., the number of the nodes and the node strength distribution) differ completely. Specifically, the number of nodes (M) are 100, 40, 440, and 554, respectively, all which are fewer than the number of fluctuation modes (i.e., $\widehat{M} = (1000-5) + 1 = 996$). This is the case because many fluctuation modes are repeated, which indicates that there are no new and different fluctuation modes in many of the time windows.Fig. 7(a) shows the relationship between the number of network nodes (M) and the time series data size (N). Note that as the sample data size (N) increases, the number of nodes (M) also slowly increases, and when the sample data size (N) reaches a certain value the number of nodes (M) will become stable. This suggests that we can use previous fluctuation modes to characterize the fluctuation modes appearing in the short term future. In addition, because we need to understand the transforming relationship among the nodes to understand the evolution of the time series, we examine how parameters r, k, and L of DFN affect the number of nodes. Fig. 7(b) shows the evolving relationship between the number of nodes and the threshold r. Note that there is a complex relationship between the number of network nodes (M) and the threshold r. In a practical application, we determine the threshold r by first setting the initial threshold r_n, e.g., using Eq. (20) to calculate r_1, selecting the r threshold in the vicinity of r_n, and calculating the corresponding loss function by using different r thresholds. We then construct the optimization model

$$\min G(r) = \sum_i w_i g_i(r) s.\ t.\ \ g_i(r) \leqslant g_i(r_n), \tag{21}$$

where g_i is the loss function and w_i is the weight. Using Eq. (21) the optimal threshold r is obtained that minimizes the loss function. Fig. 7(c) and (d) show the evolutionary relationship between the number of nodes M and parameters k and L. We find that the number of network nodes M, the number of symbols k, and the length of the sliding window L are positively

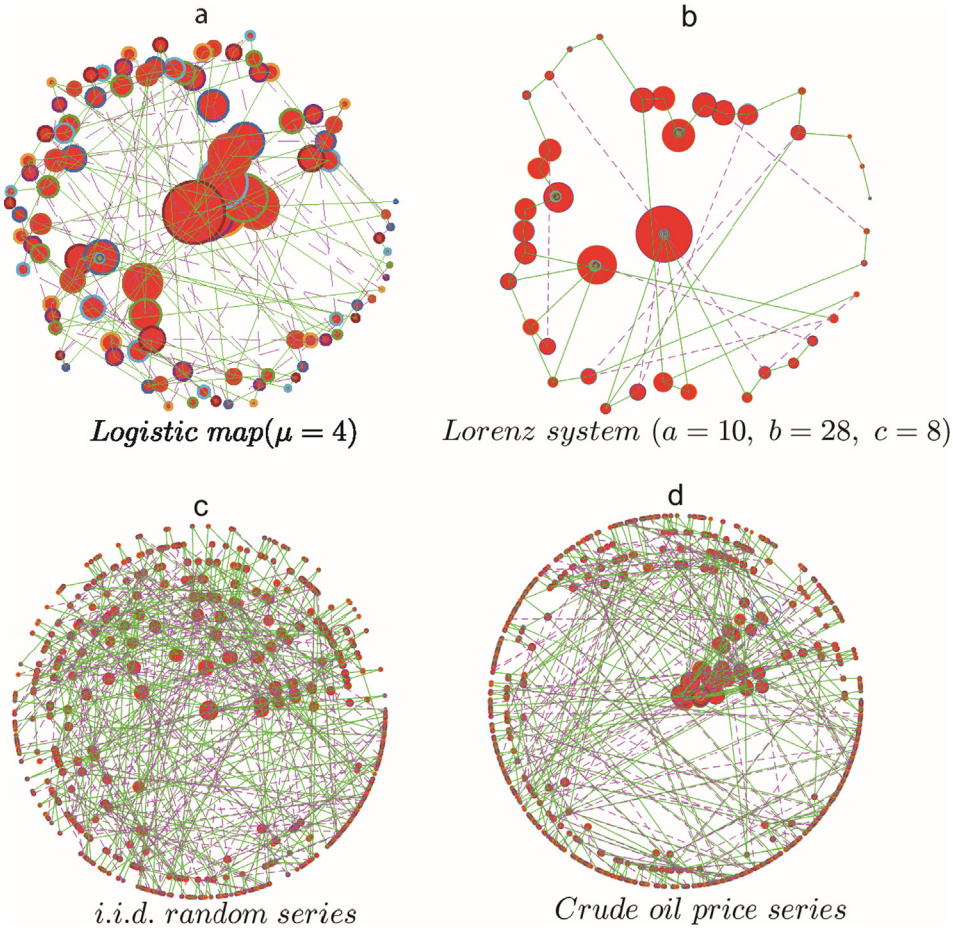

Fig. 6. Data fluctuation network (DFN) associated to different time series.

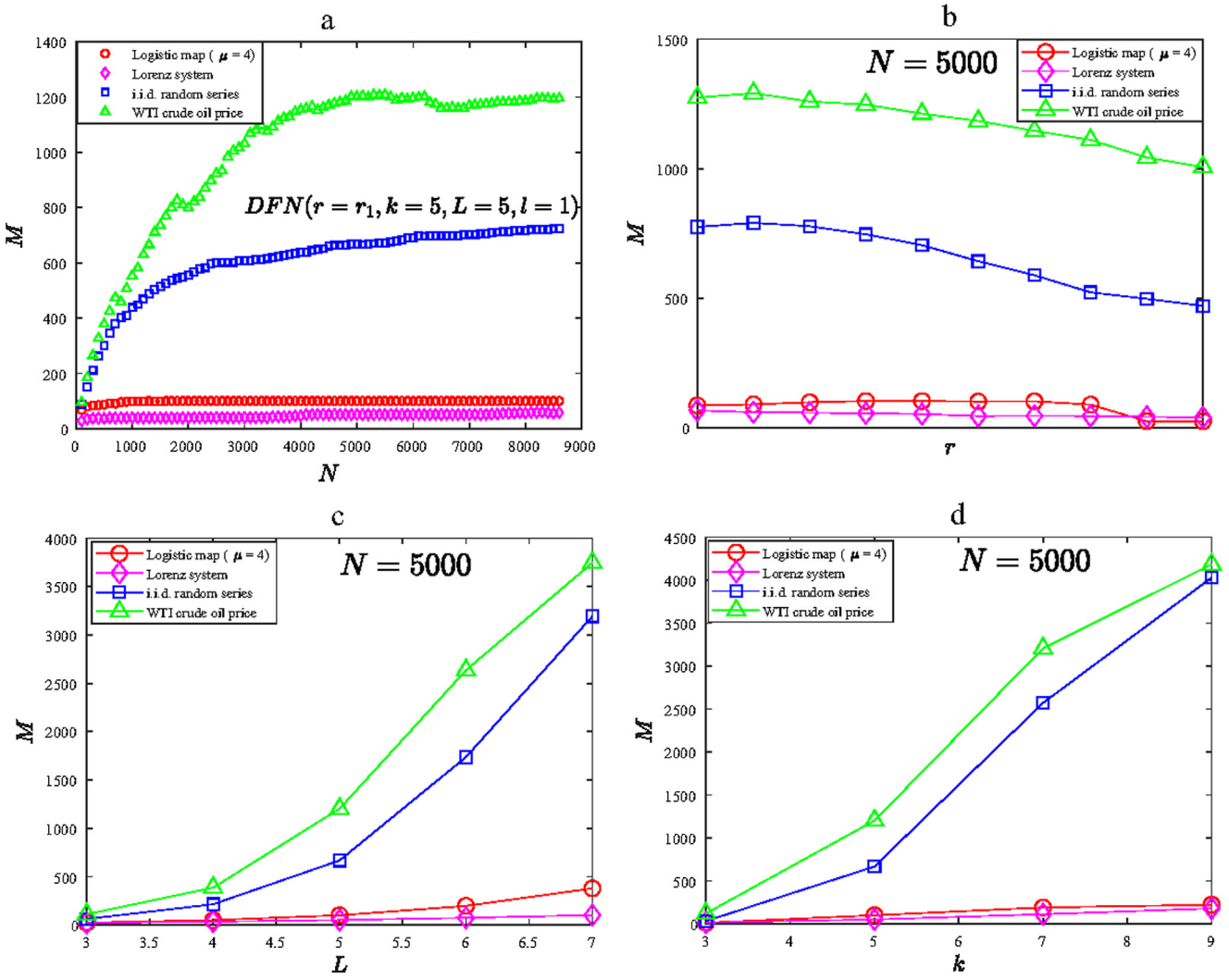

Fig. 7. The results of the parameters sensitivity analysis (a) the evolutionary relations between M and N, (b) the evolutionary relations between M and r, (c) the evolutionary relations between M and L, (d) the evolutionary relations between M and k.

correlated, i.e., as parameters k and L increase, the number of network nodes increase. Thus, the parameters k and L can be directly determined by using the characters of the time series.

4. Crude oil price forecasting result analysis

Here all the models are run 10 times using the MATLAB R2017b software package. All programs are run on a Lenovo laptop computer with an i5-4200U 1.60 GHz CPU and 4 GB of RAM. The sample data is obtained from the U.S. energy information administration (EIA) (http://www.eia.gov/). To analyze robustness three datasets are selected, i.e., daily, weekly, and monthly. To compare and analyze, in each dataset we randomly select 200 sample data for training and testing. In response to previous relevant research [57] we set at 9:1 the size ratio between training and testing sets. Using the number of the sample data, we set parameters $k = 3$, $r = 0$, $L = 5$, and $l = 1$ to build the DFN, and use all the elements in set $V_{i\to j}^{t+1}$ to determine the future fluctuations of the target node. The BPNN, RBFNN, and ELM are standard two-layer AI network models that have a hidden layer and an output layer. Note that a small number of hidden neurons causes inaccuracies in the correlation between inputs and outputs, and that a large number produces local optimums. Hastie et al. [57] find that the typical number of nodes is in the 5 to 100 range, and thus using cross validation is unnecessary. Thus, the parameters are set as follows. For BPNN we set the number of nodes in the hidden layer to the default value of 'newff' command in MATLAB, and we set the other training parameters net.trainParam.epochs = 1000, net.trainParam.goal = 1e-6, and net.trainParam.lr = 0.01. For RBFNN we set the number of nodes in the hidden layer to 90 and the radial basis function to the Gaussian function. For ELM we set the number of nodes in the hidden layer to 8.

4.1. WTI crude oil price forecasting

4.1.1. Daily crude oil price forecasting

The daily prices from the Cushing, Oklahoma Crude Oil Future Contract 1 (Dollars per Barrel) from 4 April 1983 to 31 October 2017 are used as sample data. From these data, to verify how capable the DFN-AI models are of being generalized, we randomly select 200 sample data and use the previous 180 sample data (90%) as training samples and the remaining 20 sample data (10%) as testing samples. The original training samples are selected in 10 different periods. Fig. 8(a) and (b) show the original training samples and the corresponding DFNs. Fig. 8(c) and (d) show the testing sample values of the

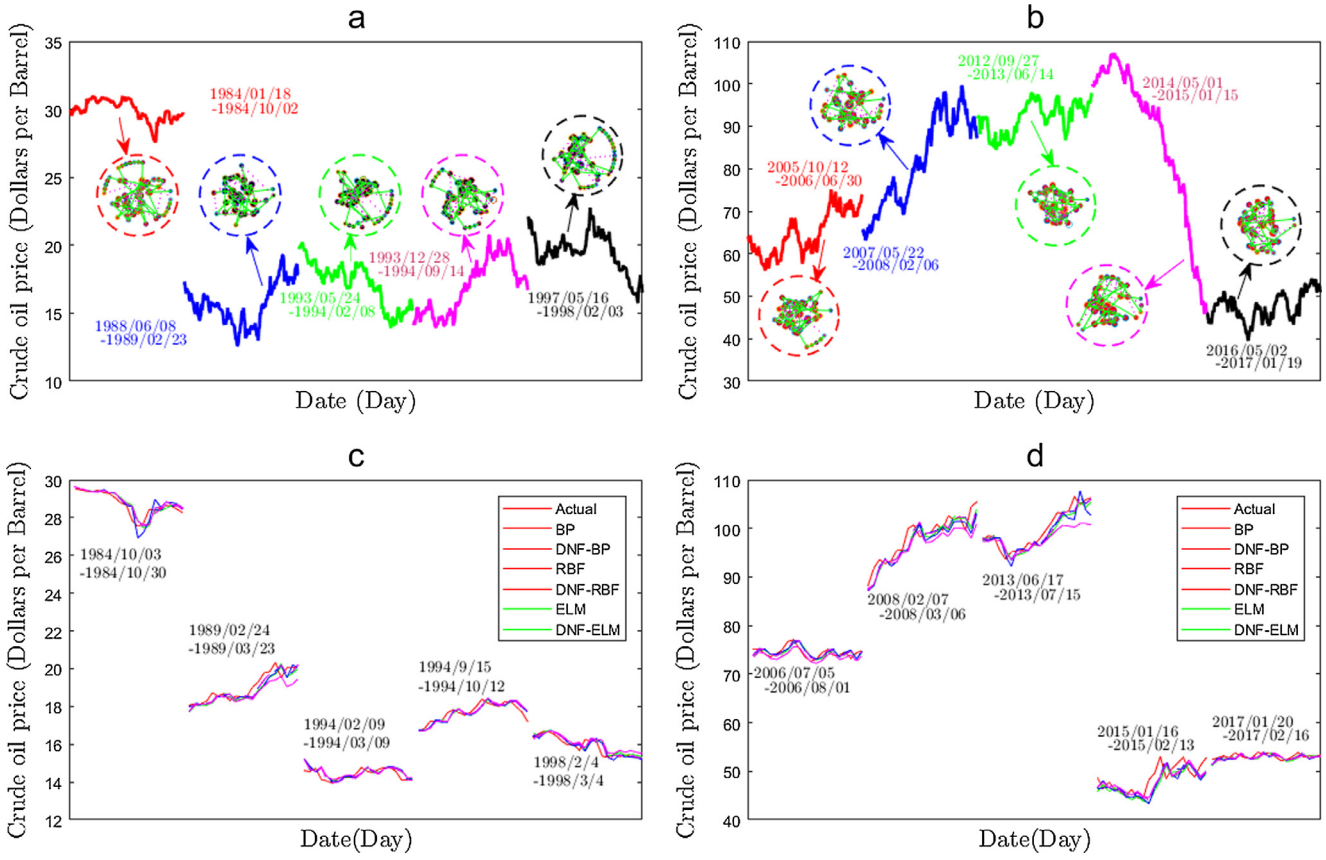

Fig. 8. The daily sample data and forecast results: (a, b) the original training samples and the DFNs mapped from these sample data. (c, d) Actual testing samples values and predicted series.

crude oil prices in different periods and the forecasts of each model. Table 2 compares the forecasting performances of the six methods, and the last line in each period shows the average running time of each model in the period. The last row of Table 2 shows the mean value of each model in all periods. The values in boldface are the best MAPE, RMSE and Dstat performances among the six models.

Table 2 compares the DFN-BP, DFN-RBF, and DFN-ELM hybrid models with their respective BPNN, RBFNN, and ELM single counterparts. Note that the directional and level prediction accuracies of the hybrid models are better than those of the single AI benchmark models. The average MAPE values of BPNN (0.01566), RBFNN (0.1548), and ELM (0.1740) are much higher than the average MAPE values of DFN-BP (0.01359), DFN-RBF (0.0137), and DFN-ELM (0.01360), and the DFN-BP model has the lowest MAPE. Similarly, the average RMSE values of BPNN (0.94848), RBFNN (0.98419), and ELM (1.12115) are much higher than the average RMSE values of DFN-BP (0.85213), DFN-RBF (0.86065), and DFN-ELM (0.85444), and the DFN-BP model has the lowest RMSE.

The directional prediction accuracy of the average Dstat values of BPNN (0.47500), RBFNN (0.50500) and ELM (0.43500) is lower than the average Dstat values of DFN-BP (0.68000), DFN-RBF (0.69000), and DFN-ELM (0.71500). Note that the hybrid models achieve a higher Dstat than their corresponding single AI models, and that the DFN-ELM model has highest Dstat. All of this indicates the proposed DFN-AI technique is a promising tool for forecasting crude oil prices. This is because the traditional AI models (i.e., BPNN, RBFNN and ELM) are unable to extract, organize, and discriminate the information from the original data [44]. Because there are many fluctuation features in the crude oil price series, the traditional AI models cannot learn a useful representation, and their sample forecast is thus inferior. In contrast, the DFN-AI models use a complex network oil price algorithm to extract the fluctuation features of the crude oil price series, and thus they improve the predictive performance by reconstructing the data using the extracted information. Thus, daily observations tell us that the forecasted results of DFN-AI models are more reasonable and more accurate than the corresponding single AI models. In addition, the DFN-AI models are able to generalize when forecasting crude oil prices, i.e., their forecasting power is not affected by the training and testing sample selection.

4.1.2. *Weekly crude oil price forecasting*

Previous studies assume data frequency to be an important factor that affects the accuracy of crude oil price forecasting [1–31]. Thus we use weekly data to examine the forecasting accuracy of DFN-AI models. Fig. 9(a) and (b) show the original weekly training samples and the corresponding DFNs. As in the daily sample data, we select the original weekly training samples from ten different periods. Fig. 9(c) and (d) show the crude oil price forecasts of each model of the testing samples in the different periods. Table 3 lists the forecasting performance results of the six methods.

Table 3 compares the DFN-AI models with their respective single counterparts. Note that the weekly observations clearly indicate that the DFN-AI models are more accurate in both their directional and level predictions than the single benchmark models. The average MAPE values of BPNN (0.02799), RBFNN (0.03072) and ELM (0.03015) are higher than the average MAPE values of DFN-BP (0.02610), DFN-RBF (0.02687), and DFN-ELM (0.02603), and the DFN-ELM model has the lowest MAPE. The average RMSE values of BPNN (1.76251), RBFNN (1.87347) and ELM (1.77927) are higher than the average RMSE values of DFN-BP (1.71515), DFN-RBF (1.73190), and DFN-ELM (1.70225), and the DFN-ELM model has the lowest RMSE. For the directional

Table 2
The errors and elapsed times of daily WTI crude oil price forecasting using the six methods.

Training	Testing	Criteria	BPNN	DFN-BP	RBFNN	DFN-RBF	ELM	DFN-ELM
1984/01/18–1984/10/02	1984/10/03–1984/10/30	MAPE	0.00762	0.00640	0.00874	0.00617	0.00698	**0.00594**
		RMSE	0.32236	0.29254	0.33550	0.28044	0.29118	**0.27305**
		Dstat	0.30000	0.70000	0.50000	0.75000	0.55000	**0.80000**
		Time(s)	5.30200	36.74100	3.43500	15.27500	1.00000	2.82900
1988/06/08–1989/02/23	1989/02/24–1989/03/23	MAPE	0.01567	**0.01243**	0.01438	0.01279	0.02008	0.01249
		RMSE	0.36350	**0.30829**	0.35877	0.31448	0.50126	0.31017
		Dstat	0.40000	**0.70000**	0.40000	**0.70000**	0.30000	**0.70000**
		Time(s)	5.20800	33.06400	3.44100	15.36200	0.96900	2.81500
1993/05/24–1994/02/08	1994/02/09–1994/03/09	MAPE	0.01483	**0.01247**	0.01550	0.01276	0.01442	0.01261
		RMSE	0.28055	0.26285	0.28203	0.26627	0.27137	**0.25732**
		Dstat	0.50000	**0.65000**	0.30000	0.55000	0.50000	**0.65000**
		Time(s)	7.28000	39.09000	3.30800	15.83400	1.05600	2.98600
1993/12/28–1994/09/14	1994/09/15–1994/10/12	MAPE	0.01098	0.01064	0.01034	**0.01033**	0.01170	0.01038
		RMSE	0.24365	0.24022	0.23447	0.23875	0.25587	**0.23808**
		Dstat	0.55000	0.75000	0.70000	**0.80000**	0.45000	**0.80000**
		Time(s)	5.84300	37.62600	3.46400	44.16300	1.06300	3.06300
1997/05/16–1998/02/03	1998/2/4–1998/03/04	MAPE	0.01225	0.01045	0.01177	**0.00997**	0.01534	0.01036
		RMSE	0.27124	0.25745	0.25661	**0.25452**	0.30291	0.25600
		Dstat	0.45000	**0.75000**	0.60000	0.70000	0.35000	0.70000
		Time(s)	6.11300	37.60900	3.40900	43.74900	3.12000	2.88600
2005/10/12–2006/06/30	2006/07/05–2006/08/01	MAPE	0.01171	0.01029	0.01060	**0.01011**	0.01301	0.01024
		RMSE	1.00221	0.92563	0.95441	0.92237	1.14353	**0.91243**
		Dstat	0.60000	0.75000	0.65000	0.75000	0.40000	**0.80000**
		Time(s)	5.26600	34.28100	3.33400	14.91300	0.95300	2.84700
2007/05/22–2008/02/06	2008/02/07–2008/03/06	MAPE	0.01807	**0.01603**	0.01952	0.01631	0.02244	0.01641
		RMSE	2.22894	**2.06907**	2.38964	2.09595	2.78182	2.09777
		Dstat	0.60000	**0.75000**	0.35000	0.70000	0.40000	**0.75000**
		Time(s)	5.14100	34.52800	3.45000	15.09800	0.92600	2.82900
2012/09/27–2013/06/14	2013/6/17–2013/07/15	MAPE	0.01291	**0.01105**	0.01595	0.01106	0.02258	0.01124
		RMSE	1.56477	**1.40429**	2.04951	1.40391	2.89178	1.43652
		Dstat	0.40000	0.55000	0.35000	0.60000	0.40000	**0.65000**
		Time(s)	5.07800	35.15500	3.41000	15.84300	1.37500	3.06400
2014/05/01–2015/01/15	2015/1/16–2015/02/13	MAPE	0.04152	0.03659	0.03783	0.03794	0.03759	**0.03642**
		RMSE	2.51419	2.13464	2.32341	2.20231	2.12963	**2.12610**
		Dstat	0.45000	0.55000	0.50000	**0.60000**	0.45000	**0.60000**
		Time(s)	5.12600	34.12700	3.09400	15.49000	0.95300	2.89400
2016/05/02–2017/01/19	2017/01/20–2017/02/16	MAPE	0.01102	**0.00956**	0.01017	0.00991	0.00988	0.00990
		RMSE	0.69340	**0.62634**	0.65759	0.62753	0.64219	0.63693
		Dstat	0.50000	0.65000	0.70000	**0.75000**	0.55000	0.70000
		Time(s)	5.11100	33.50500	3.12600	15.12800	0.93800	2.86000
Average value		MAPE	0.01566	**0.01359**	0.01548	0.01374	0.01740	0.01360
		RMSE	0.94848	**0.85213**	0.98419	0.86065	1.12115	0.85444
		Dstat	0.47500	0.68000	0.50500	0.69000	0.43500	**0.71500**
		Time(s)	5.54680	35.57260	3.34710	15.26960	1.23530	2.90730

(The value in boldface represents the best performance amongst 6 models in terms of MAPE, RMSE and Dstat.)

prediction accuracy, the average Dstat values of BP (0.52000), RBF (0.53000) and ELM (0.49500) are lower than the average Dstat values of DFN-BP (0.63000), DFN-RBF (0.645000), and DFN-ELM (0.64500), and the DFN-ELM model has the highest Dstat. This clearly indicates that data frequency is a robust factor in our new DFN-AI crude oil price forecasting method.

4.1.3. Monthly crude oil price forecasting

To further test the robustness of our proposed DFN-AI forecasting method, we examine monthly observations. To take into account structural breaks in the data when examining the forecasting performance, we use crude oil prices from February 1994 to January 2009 and from December 1999 to November 2014 for our original training data and test them with monthly observations from February 2009 to September 2010 and from December 2014 to July 2016, respectively. We find that the crude oil prices in these periods have structural breaks [1,18,41]. Outside of these two sample periods, three other sample periods are also selected, i.e., June 1987 to January 2004, February 1989 to September 2005, and December 1999 to July 2016. Fig. 10(a) shows the selected original training samples and the corresponding DFNs. Fig. 10(b) shows the testing sample crude oil price values in different periods and the forecasts provided by each model. Table 4 lists the forecasting performance results of the six methods.

Table 4 lists and compares the DFN-AI model results with their respective single counterparts. Note that, based on monthly observations, the accuracy of both the directional and level predictions of the DFN-AI models is better than their single benchmark counterparts. With regard to level prediction accuracy, the average MAPE values of BPNN (0.07647), RBFNN (0.10432), and ELM (0.10382) are higher than the average MAPE values of DFN-BP (0.07003), DFN-RBF (0.07788), and DFN-ELM (0.06916), and the DFN-ELM model has the lowest MAPE. The average RMSE values of BPNN (4.60547), RBFNN (6.52349) and ELM (6.26923) are higher than the average RMSE values of DFN-BP (4.25353), DFN-RBF (4.66344), and DFN-ELM (4.17084), and the DFN-

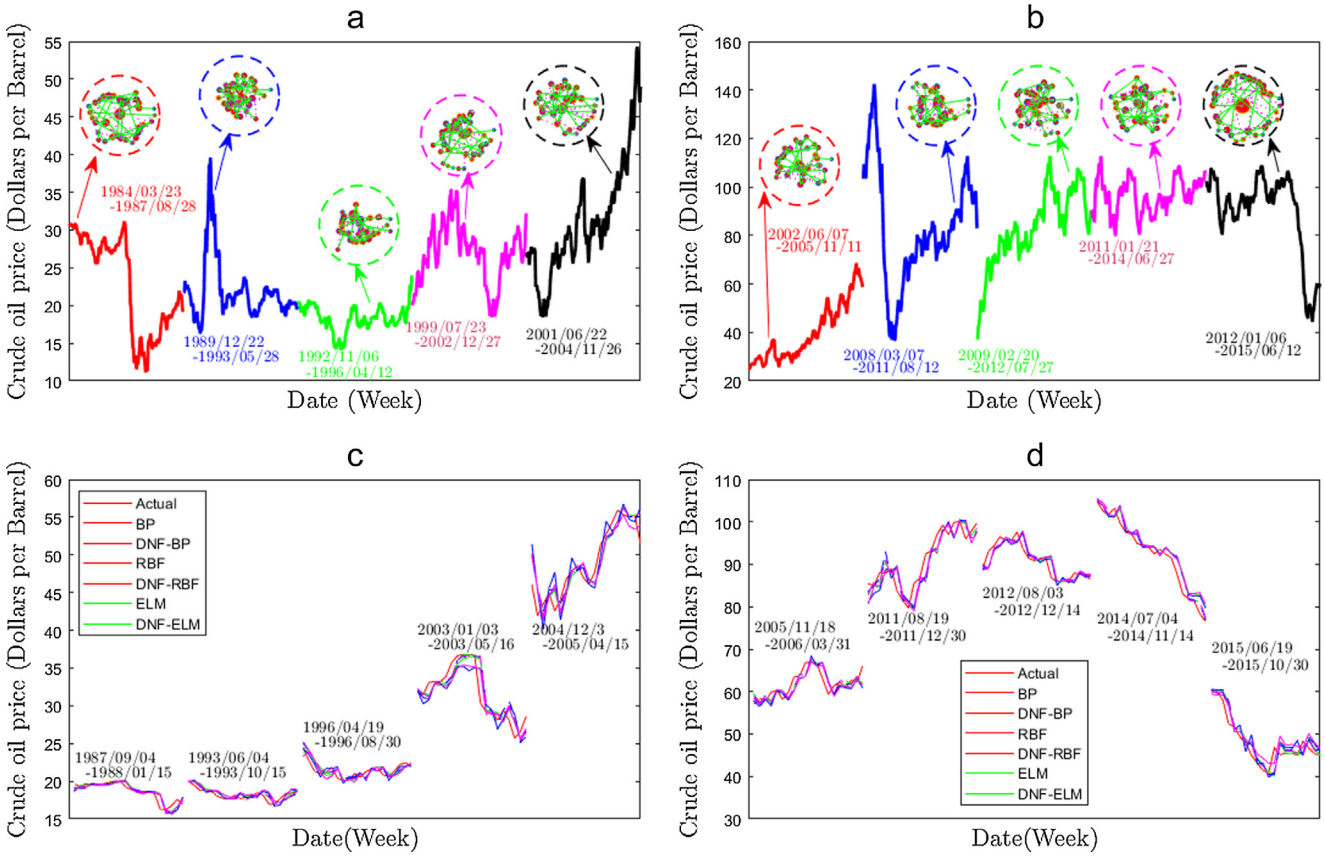

Fig. 9. The weekly sample data and forecast results: (a, b) the original training samples and the DFNs mapped from these sample data (c, d) Actual testing samples values and predicted series.

ELM model has the lowest RMSE. With regard to directional prediction accuracy, the average Dstat values of BPNN (0.45000), RBFNN (0.48000) and ELM (0.49000) are lower than the average Dstat values of DFN-BP (0.62000), DFN-RBF (0.600000), and DFN-ELM (0.63000), and the DFN-ELM model has the highest Dstat. This clearly indicates that our proposed DFN-AI crude oil price forecasting method is more robust with respect to data frequency and structural breaks.

This brings us to four conclusions. (i) The proposed DFN-AI models, i.e., the DFN-BP, DFN-RBF, and DFN-ELM, yield the best directional and level predictions. This is the case because a complex network analysis algorithm of crude oil prices can extract their fluctuation features and, using the extracted information, reconstruct the data and improve predictive model performance. (ii) The proposed DFN-AI models are able to generalize the results of their crude oil price forecasting, i.e., their forecasting power is not sensitive to training and testing sample selection. (iii) The proposed DFN-AI models are robust with respect to the data frequency and structural breaks. (iv) Although the last rows of Tables 2–4 indicate that the average running time of the proposed DFN-AI models has a higher computational cost than the corresponding single models, this is disappearing as a concern because computing power is rapidly increasing and parallel computing hardware now in common use.

4.2. Diebold-Mariano (DM) test

In using the DM test to statistically confirm our conclusions, the DMS value of Eq. (19) and the *p*-value are used to measure how much the test model is an improvement over the benchmark model. Table 5 lists the corresponding DMS values and *p*-values (in brackets). Note that the *p*-values of the DFN-AI forecasting models are over 10% smaller than those of their single benchmarks in the three cases of crude oil price data. This indicates that data reconstruction improves forecasting with a confidence level of 90%, i.e., the DFN-AI models are statistically more effective than their corresponding single models. Note that because the *p*-values are above 10% neither the three DFN-AI models (i.e., DFN-BP, DFN-RBF and DFN-ELM) nor the three single AI models (i.e., BPNN, RBFNN and ELM) are unmistakably superior.

5. Conclusion

This paper has proposed a novel hybrid prediction method by combining a complex network time series analysis and artificial intelligence algorithms. A complex network analysis of a time series is first performed as a preprocessor of the original crude oil price data to extract the fluctuation features, and then reconstruct the original data. Then an artificial intelligence tool is employed to model the reconstructed original data and gain a final prediction.

We first analyze the sensitivity of the data fluctuation parameters and then test the performance of the new hybrid method (DFN-AI) with respect to such factors as random sample selection, sample frequency, and sample structural breaks. From the empirical analysis, we draw four conclusions. (1) A complex network analysis algorithm of crude oil price can be used to extract the fluctuation features of the crude oil price and improve the predictive performance of traditional AI models by reconstructing the data using this extracted information. (2) The proposed DFN-AI models (DFN-BP, DFN-RBF, and DFN-ELM) perform significantly better than the traditional models in predicting both direction and level, indicating their ability to model nonlinear patterns

Table 3
The errors and elapsed times of weekly WTI crude oil price forecasting using the six methods.

Training	Testing	Criteria	BPNN	DFN-BP	RBFNN	DFN-RBF	ELM	DFN-ELM
1984/03/23–1987/08/28	1987/09/04–1988/01/15	MAPE	0.02360	**0.02327**	0.02576	0.02618	0.02566	0.02339
		RMSE	0.64594	**0.64113**	0.70314	0.69752	0.64395	0.64214
		Dstat	0.50000	0.55000	0.40000	**0.60000**	0.45000	0.50000
		Time(s)	5.18800	33.59600	3.11000	14.71100	1.01600	2.84800
1989/12/22–1993/05/28	1993/06/04–1993/10/15	MAPE	0.02590	**0.01827**	0.02182	0.01986	0.02688	0.01835
		RMSE	0.56671	**0.41464**	0.52458	0.44756	0.59137	0.42591
		Dstat	0.35000	**0.60000**	0.50000	0.55000	0.40000	**0.60000**
		Time(s)	5.12500	33.71600	3.06300	14.94100	0.92200	2.82900
1992/11/06–1996/04/12	1996/04/19–1996/08/30	MAPE	0.03023	0.02810	0.02677	**0.02606**	0.03334	0.02693
		RMSE	0.78025	0.76047	0.75036	**0.70696**	0.85774	0.73953
		Dstat	0.55000	0.65000	0.75000	**0.80000**	0.45000	0.75000
		Time(s)	5.23500	33.36100	3.11000	14.80000	0.95300	2.86100
1999/07/23–2002/12/27	2003/01/03–2003/05/16	MAPE	0.03787	**0.03686**	0.05033	0.04169	0.04253	0.03836
		RMSE	1.69630	1.75929	1.89560	1.90146	**1.65495**	1.77796
		Dstat	0.50000	**0.65000**	0.50000	0.40000	0.45000	0.60000
		Time(s)	5.12700	33.58400	3.07800	14.85200	0.90600	2.79700
2001/06/22–2004/11/26	2004/12/03–2005/04/15	MAPE	0.03579	0.03393	0.04481	0.03242	0.03545	**0.03305**
		RMSE	2.05170	2.01826	2.61509	**2.00607**	2.01482	2.01028
		Dstat	0.65000	0.70000	0.55000	0.70000	0.65000	**0.75000**
		Time(s)	5.04800	33.63700	3.09500	14.89500	0.93800	2.82900
2002/06/07–2005/11/11	2005/11/18–2006/03/31	MAPE	0.02833	0.02860	0.02894	**0.02674**	0.02770	0.02741
		RMSE	2.15536	2.12314	2.27032	**2.04847**	2.08595	2.06149
		Dstat	0.60000	**0.65000**	0.55000	**0.65000**	0.55000	**0.65000**
		Time(s)	5.06900	33.56800	3.06300	14.66200	0.93700	2.82900
2008/03/07–2011/08/12	2011/08/19–2011/12/30	MAPE	0.02766	0.02664	0.03019	**0.02638**	0.02717	0.02645
		RMSE	3.13763	**2.98420**	3.26857	3.08068	3.12836	2.98981
		Dstat	0.50000	0.65000	0.55000	**0.70000**	0.50000	0.65000
		Time(s)	5.12600	33.51200	3.07900	14.86300	0.93700	2.81300
2009/02/20–2012/07/27	2012/08/03–2012/12/14	MAPE	0.01461	**0.01408**	0.01503	0.01483	0.01458	0.01430
		RMSE	1.94809	1.99358	**1.88318**	1.93221	1.97159	1.95198
		Dstat	0.50000	0.60000	0.55000	**0.75000**	0.55000	0.65000
		Time(s)	5.09500	33.46800	3.06300	14.77100	0.93800	2.87500
2011/01/21–2014/06/27	2014/07/04–2014/11/14	MAPE	0.02085	0.01768	0.01985	**0.01701**	0.02169	0.01752
		RMSE	2.29797	2.11034	2.23731	**2.06173**	2.40837	2.10342
		Dstat	0.45000	0.55000	0.40000	**0.70000**	0.45000	**0.70000**
		Time(s)	5.08400	33.53800	3.06400	14.65200	0.92200	2.76600
2012/01/06–2015/06/12	2015/06/19–2015/10/30	MAPE	0.03502	**0.03358**	0.04372	0.03758	0.04654	0.03453
		RMSE	2.34512	2.34650	2.58654	2.43634	2.43559	**2.32001**
		Dstat	0.60000	**0.70000**	0.55000	0.60000	0.50000	0.60000
		Time(s)	5.07200	33.69800	3.07800	14.86300	0.93800	2.81300
Average value		MAPE	0.02799	0.02610	0.03072	0.02687	0.03015	**0.02603**
		RMSE	1.76251	1.71515	1.87347	1.73190	1.77927	**1.70225**
		Dstat	0.52000	0.63000	0.53000	**0.64500**	0.49500	**0.64500**
		Time(s)	5.11690	33.56780	3.08030	14.80100	0.94070	2.82600

(The value in boldface represents the best performance amongst 6 models in terms of MAPE, RMSE and Dstat.)

hidden in crude oil prices. (3) The forecasting performance of the proposed DFN-AI model is excellent irrespective of random sample selection, sample frequency, or sample structural breaks, indicating its robustness and reliability. (4) Although the average running time of the proposed DFN-AI models has a higher computational cost than that of the corresponding single models, this is disappearing as a concern because computing power is rapidly increasing and parallel computing hardware now in common use.Thus the DFN-AI crude oil price forecasting method is a useful tool for investors and analysts evaluating price trends and forecasting crude oil prices. For example, we can use a complex network analysis algorithm to map crude oil prices on a directed and weighted data fluctuation network (DFN) using the topological structure of the DFN (e.g., node strength, cluster coefficient, and node betweenness) in order to characterize the fluctuation characteristics of crude oil prices. Specifically, we can use the link relations among the nodes to uncover the fluctuation trends of crude oil prices. Thus, our new method can be used to capture the complex dynamic behavior of crude oil prices. For our oil price prediction problem, by mapping time-series data into data fluctuation network, the noise in the data was removed and the underlying tendencies were revealed. This enables to resolve the complexity and irregularity of oil price prediction problem caused by its intrinsic dynamics, and results in more accurate prediction than that offered by the traditional prediction models. Note that we set 200 sample data as an example for training and testing, moreover, we can set different scales of sample size depending on the needs of the analysis. Here we discuss how what is the effect of increasing the training set on the predicted results? For the sake of simplicity, we fixed the model parameters set in the above paper, only changed the training set size. Fig. 11 shows the prediction results of the single AI models and DFN-AI models under different training set size. It can be seen that in Fig. 11, under each of these single AI and DFN-AI models, both the level accuracy indicators MAPE and RMSE move downward and then gradually go stable, while the direction accuracy indicator Dstat goes upward and then turns stable. Such tendencies indicate that both the level and direction prediction accuracies of these single AI and DFN-AI models improve as sample size increases.

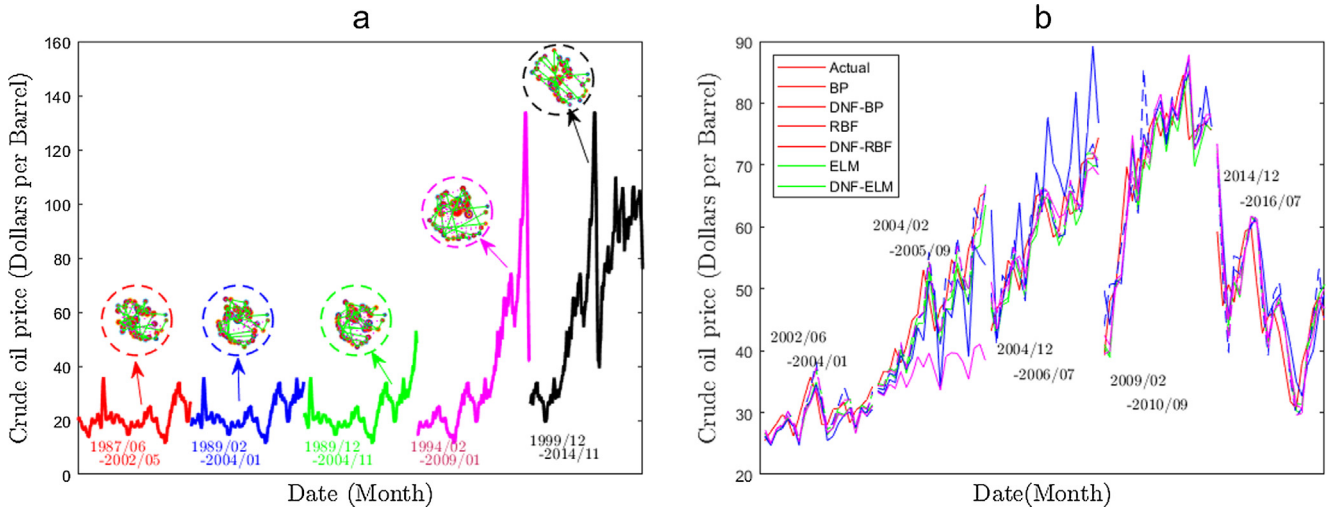

Fig. 10. The monthly sample data and forecast results: (a) the original training samples and the DFNs mapped from these sample data. (b) Actual testing samples values and predicted series.

Table 4
The errors and elapsed times of monthly WTI crude oil price forecasting using the six methods.

Training	Testing	Criteria	BPNN	DFN-BP	RBFNN	DFN-RBF	ELM	DFN-ELM
1987/06–2002/05	2002/6–2004/01	MAPE	0.07206	0.06731	0.07564	0.06816	0.07061	**0.06649**
		RMSE	2.42456	2.38523	2.61251	2.37701	2.39976	**2.35643**
		Dstat	0.40000	0.55000	0.50000	**0.65000**	0.40000	0.5500
		Time(s)	5.25400	34.68700	3.15700	16.24100	0.92200	2.78200
1989/02–2004/01	2004/02–2005/09	MAPE	0.07468	**0.06370**	0.11056	0.07925	0.21223	0.06497
		RMSE	4.61656	**3.73852**	7.35495	4.43963	13.24985	3.79178
		Dstat	0.30000	**0.60000**	0.30000	0.55000	0.30000	0.55000
		Time(s)	5.20400	33.31100	3.13000	16.58500	0.93800	2.81400
1989/12–2004/11	2004/12–2006/07	MAPE	0.05960	**0.05604**	0.12910	0.06974	0.05835	0.05621
		RMSE	4.22660	**3.86493**	9.84207	4.61297	3.95064	3.87414
		Dstat	0.40000	**0.75000**	0.65000	0.55000	0.55000	0.75000
		Time(s)	5.17300	33.63400	3.11000	17.23500	0.93700	3.03200
1994/02–2009/01	2009/02–2010/09	MAPE	0.07065	0.06586	0.07735	0.06558	0.06817	**0.06101**
		RMSE	5.82473	5.60917	5.98303	5.80642	5.66098	**5.17863**
		Dstat	0.50000	0.55000	0.55000	0.55000	0.55000	**0.65000**
		Time(s)	5.07900	33.74300	3.10900	16.61100	0.91000	2.82800
1999/12–2014/11	2014/12–2016/7	MAPE	0.10538	0.09723	0.12895	0.10668	0.10975	**0.09711**
		RMSE	5.93489	5.66978	6.82489	6.08115	6.08490	**5.65323**
		Dstat	0.65000	0.65000	0.40000	**0.70000**	0.65000	0.65000
		Time(s)	5.08400	33.51300	3.09400	16.29000	0.98400	2.84600
Average value		MAPE	0.07647	0.07003	0.10432	0.07788	0.10382	**0.06916**
		RMSE	4.60547	4.25353	6.52349	4.66344	6.26923	**4.17084**
		Dstat	0.45000	0.62000	0.48000	0.60000	0.49000	**0.63000**
		Time(s)	5.15880	33.77760	3.12000	16.59240	0.93820	2.86040

(The value in boldface represents the best performance amongst 6 models in terms of MAPE, RMSE and Dstat.)

Comparing the prediction results of the single AI models and DFN-AI models, we find that the proposed DFN-AI models (DFN-BP, DFN-RBF, and DFN-ELM) perform significantly better than the single AI (BPNN, RBFNN, and ELM) models in predicting both direction and level under different training data size. Note that all the results in Fig. 11 are obtained under the fixed parameters set in Section 4, in practical application, in order to achieve higher prediction accuracy, we need to set appropriate parameters of DFN-AI models according to the size and structure characteristics of the sample data. For example, if the sample data size is large, parameter k and L can be set to larger values and parameter α can be set to smaller value.

In addition to examining crude oil price data, our DFN-AI method can also address other forecasting tasks, especially when complex, irregular, and highly nonlinear data are involved. In practical application, the basic calculation of the method is: first perform DFN as a preprocessor for the original data to reconstruct the data, and then use a certain powerful AI tool such as SVM, deep neural networks (DNN) to conduct prediction for the reconstructed data. In the process of building the DFN-AI model, choosing suitable parameters (i.e., r, k, and L) to build the data fluctuation network determines the quality of data reconstruction and the predictive accuracy of the model. In future studies, we will do further research on how to determine the optimal parameters. Note that when we reconstruct the training data in this paper, we use all the neighbor nodes of the target node. There are other topological indicators for describing the topological structure of a data fluctuation network, such as K-core centrality, the H index, and community structure. Further research is needed to make use of these topological indicators when reconstructing training data. Because the volatility of crude oil prices is complicated, future research could combine the latest complex network theory, an econometric model, and

Table 5
DM test results for DFN-AI models and their single benchmark models.

Data type	Tested model	Reference model				
		DFN-RBF	DFN-ELM	BPNN	RBFNN	ELM
Daily data	DFN-BP	−1.16810 **(0.13640)**	−0.43311 **(0.33760)**	−2.66890 **(0.01284)**		
	DFN-RBF		0.71283 **(0.75300)**		−1.92100 **(0.04346)**	
	DFN-ELM					−1.90400 **(0.04236)**
	BPNN				−0.63057 **(0.27200)**	−1.17000 **(0.13600)**
	RBFNN					−1.17680 **(0.12692)**
Weekly data	DFN-BP	−0.68571 **(0.25510)**	1.63160 **(0.93140)**	−1.82150 **(0.04863)**		
	DFN-RBF		1.50070 **(0.91620)**		−2.37900 **(0.02065)**	
	DFN-ELM					−2.07670 **(0.03381)**
	BPNN				−0.81490 **(0.15146)**	−0.87941 **(0.20100)**
	RBFNN					1.31400 **(0.88930)**
Monthly data	DFN-BP	−1.03130 **(0.12864)**	0.93865 **(0.79950)**	−2.48630 **(0.03388)**		
	DFN-RBF		3.83510 **(0.99070)**		−1.89920 **(0.06518)**	
	DFN-ELM					−1.83920 **(0.06910)**
	BPNN				−1.05030 **(0.12697)**	−0.95408 **(0.19700)**
	RBFNN					0.13606 **(0.55080)**

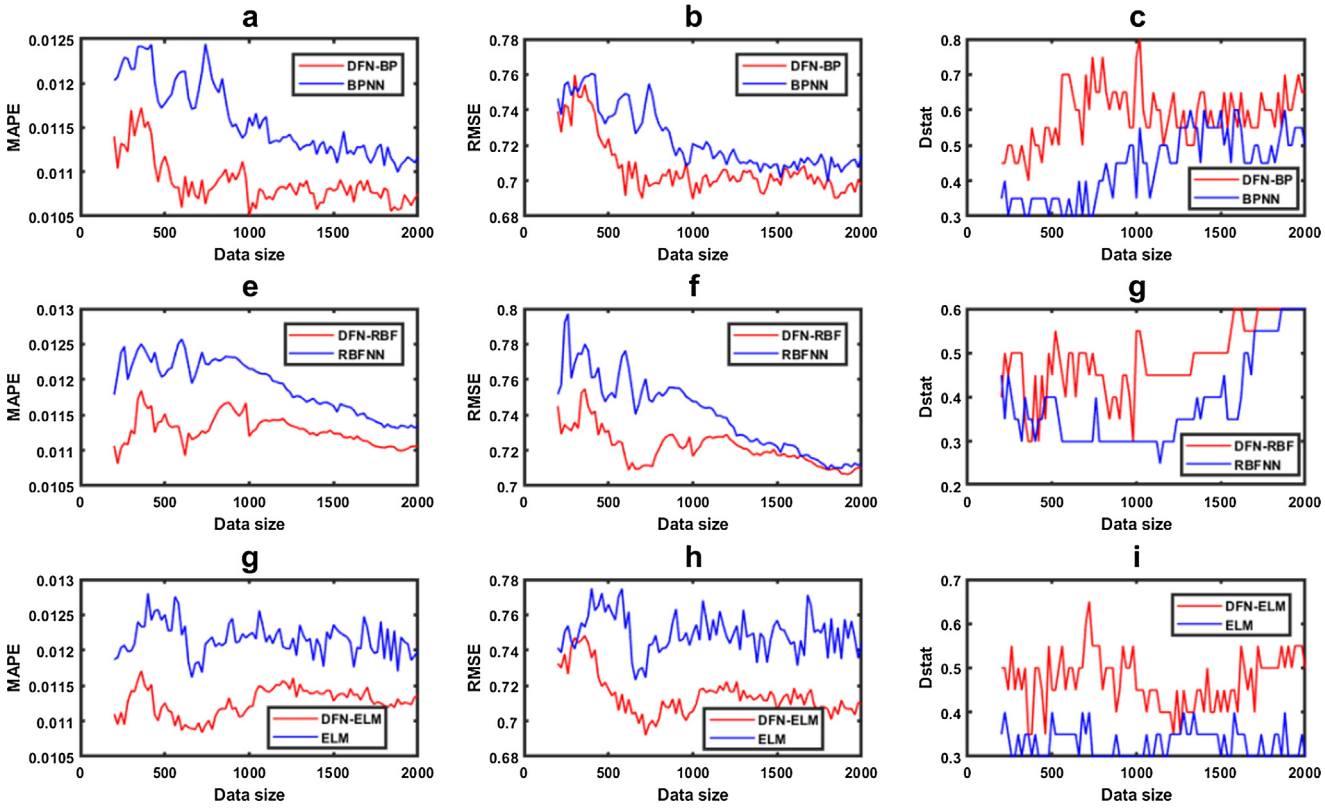

Fig. 11. The prediction results of the single AI models and DFN-AI models under different training set size.

an artificial intelligence algorithm to construct new hybrid prediction models and further enhance forecasting accuracy.

Acknowledgments

The Research was supported by the following foundations: The National Natural Science Foundation of China (71503132, 71690242, 91546118, 11731014, 71403105, 61403171, 61603011), Qing Lan Project of Jiangsu Province (2017), University Natural Science Foundation of Jiangsu Province (14KJA110001), Jiangsu Center for Collaborative Innovation in Geographical Information Resource Development and Application, the program of China Scholarship Council (No. 201606770023). China Postdoctoral Science Foundation (2016M590973), Shanxi Postdoctoral Research Foundation. The Boston University Center for Polymer Studies is supported by NSF Grants PHY-1505000, CMMI-1125290, and CHE-1213217, by DTRA Grant HDTRA1-14-1-0017, and by DOE Contract DE-AC07-05Id14517.

References

[1] Zhang JL, Zhang YJ, Zhang L. A novel hybrid method for crude oil price forecasting. Energy Econ 2015;49:649–59.
[2] Kilian L. Not all oil price shocks are alike: disentangling demand and supply shocks in the crude oil market. Am Econ Rev 2009;99(3):1053–69.
[3] Lizardo RA, Mollick AV. Oil price fluctuations and US dollar exchange rates. Energy Econ 2010;32(2):399–408.
[4] Kilian L, Murphy DP. The role of inventories and speculative trading in the global market for crude oil. J Appl Economet 2014;29(3):454–78.
[5] Sahir MH, Qureshi AH. Specific concerns of Pakistan in the context of energy security issues and geopolitics of the region. Energy Policy 2007;35(4):2031–7.
[6] Ramsay KW. Revisiting the resource curse: natural disasters, the price of oil, and democracy. Int Organ 2011;65(3):507–29.
[7] Lanza A, Manera M, Giovannini M. Modeling and forecasting cointegrated relationships among heavy oil and product prices. Energy Econ 2005;27(6):831–48.
[8] Murat A, Tokat E. Forecasting oil price movements with crack spread futures. Energy Econ 2009;31(1):85–90.
[9] Baumeister C, Kilian L. Real-time forecasts of the real price of oil. J Bus Econ Stat 2012;30(2):326–36.
[10] Xiang Y, Zhuang XH. Application of ARIMA model in short-term prediction of international crude oil price. Trans Tech Publicat 2013;798:979–82.
[11] Sadorsky P. Modeling and forecasting petroleum futures volatility. Energy Econ 2006;28(4):467–88.
[12] Fan Y, Zhang YJ, Tsai HT, et al. Estimating 'Value at Risk'of crude oil price and its spillover effect using the GED-GARCH approach. Energy Econ 2008;30(6):3156–71.
[13] Kang SH, Kang SM, Yoon SM. Forecasting volatility of crude oil markets. Energy Econ 2009;31(1):119–25.
[14] Mohammadi H, Su L. International evidence on crude oil price dynamics: applications of ARIMA-GARCH models[J]. Energy Econ 2010;32(5):1001–8.
[15] Hou A, Suardi S. A nonparametric GARCH model of crude oil price return volatility. Energy Econ 2012;34(2):618–26.
[16] Moshiri S, Foroutan F. Forecasting nonlinear crude oil futures prices. Energy J 2006:81–95.
[17] Kaboudan MA. Compumetric forecasting of crude oil prices[C]//Evolutionary Computation, 2001. In: Proceedings of the 2001 congress on. IEEE; 2001, 1, p. 283–7.
[18] Mostafa MM, El-Masry AA. Oil price forecasting using gene expression programming and artificial neural networks. Econ Model 2016;54:40–53.
[19] Kaboli SHA, Selvaraj J, Rahim NA. Long-term electric energy consumption forecasting via artificial cooperative search algorithm. Energy 2016;115:857–71.
[20] Kaboli SHA, Fallahpour A, Selvaraj J, et al. Long-term electrical energy consumption formulating and forecasting via optimized gene expression programming. Energy 2017;126:144–64.
[21] Xie W, Yu L, Xu S, et al. A new method for crude oil price forecasting based on support vector machines. Computational Science–ICCS 2006; 2006. p. 444–51.
[22] Shin H, Hou T, Park K, et al. Prediction of movement direction in crude oil prices based on semi-supervised learning. Decis Supp Syst 2013;55(1):348–58.
[23] Yusof Y, Mustaffa Z. A review on optimization of least squares support vector machine for time series forecasting. Int J Artif Intell & Applications 2016;7(2):35–49.
[24] Zhao Y, Li J, Yu L. A deep learning ensemble approach for crude oil price forecasting. Energy Econ 2017;66:9–16.
[25] Yu L, Wang S, Lai KK. Forecasting crude oil price with an EMD-based neural network ensemble learning paradigm. Energy Econ 2008;30(5):2623–35.
[26] Jammazi R, Aloui C. Crude oil price forecasting: experimental evidence from wavelet decomposition and neural network modeling. Energy Econ 2012;34(3):828–41.
[27] Xiong T, Bao Y, Hu Z. Beyond one-step-ahead forecasting: evaluation of alternative multi-step-ahead forecasting models for crude oil prices. Energy Econ 2013;40:405–15.
[28] Yu L, Dai W, Tang L. A novel decomposition ensemble model with extended extreme learning machine for crude oil price forecasting. Eng Appl Artif Intell 2016;47:110–21.
[29] Yu L, Zhao Y, Tang L. A compressed sensing based AI learning paradigm for crude oil price forecasting. Energy Econ 2014;46:236–45.
[30] Chiroma H, Abdulkareem S, Herawan T. Evolutionary neural network model for West Texas intermediate crude oil price prediction. Appl Energy 2015;142:266–73.
[31] Wang S, Yu L, Lai KK. A novel hybrid AI system framework for crude oil price forecasting[M]//data mining and knowledge management. Berlin, Heidelberg: Springer; 2005. p. 233–42.
[32] Sang YF, Wang D, Wu JC, et al. Entropy-based wavelet de-noising method for time series analysis. Entropy 2009;11(4):1123–47.
[33] He K, Lai KK, Yen J. A hybrid slantlet denoising least squares support vector regression model for exchange rate prediction. Proc Comput Sci 2010;1(1):2397–405.
[34] De Faria EL, Albuquerque MP, Gonzalez JL, et al. Predicting the Brazilian stock market through neural networks and adaptive exponential smoothing methods. Exp Syst Appl 2009;36(10):12506–9.
[35] Nasseri M, Moeini A, Tabesh M. Forecasting monthly urban water demand using Extended Kalman Filter and Genetic Programming. Exp Syst Appl 2011;38(6):7387–95.
[36] Lacasa L, Luque B, Ballesteros F, et al. From time series to complex networks: the visibility graph. Proc Natl Acad Sci 2008;105(13):4972–5.
[37] Xu X, Zhang J, Small M. Superfamily phenomena and motifs of networks induced from time series. Proc Natl Acad Sci 2008;105(50):19601–5.
[38] Zhang J, Small M. Complex network from pseudo-periodic time series: topology versus dynamics. Phys Rev Lett 2006;96(23):238701.
[39] Wang M, Tian L. From time series to complex networks: the phase space coarse graining. Phys A: Stat Mech Its Appl 2016;461:456–68.
[40] Wang M, Tian L. Regulating effect of the energy market—Theoretical and empirical analysis based on a novel energy prices–energy supply–economic growth dynamic system. Appl Energy 2015;155:526–46.
[41] Du R, Wang Y, Dong G, et al. A complex network perspective on interrelations and evolution features of international oil trade, 2002–2013. Appl Energy 2017;196:142–51.
[42] Du R, Dong G, Tian L, et al. Spatiotemporal dynamics and fitness analysis of global oil market: based on complex network. PloS One 2016;11(10):e0162362.
[43] Wang M, Chen Y, Tian L, et al. Fluctuation behavior analysis of international crude oil and gasoline price based on complex network perspective. Appl Energy 2016;175:109–27.
[44] Wang M, Tian L, Du R. Research on the interaction patterns among the global crude oil import dependency countries: a complex network approach. Appl Energy 2016;180:779–91.
[45] Wang M, Tian L, Xu H, et al. Systemic risk and spatiotemporal dynamics of the consumer market of China. Phys A: Stat Mech Its Appl 2017;473:188–204.
[46] Chen H, Tian L, Wang M, et al. Analysis of the dynamic evolutionary behavior of American heating oil spot and futures price fluctuation networks. Sustainability 2017;9(4):574.
[47] An H, Zhong W, Chen Y, et al. Features and evolution of international crude oil trade relationships: a trading-based network analysis. Energy 2014;74:254–9.
[48] An H, Gao X, Fang W, et al. Research on patterns in the fluctuation of the co-movement between crude oil futures and spot prices: a complex network approach. Appl Energy 2014;136:1067–75.
[49] Gao X, An H, Fang W, et al. The transmission of fluctuant patterns of the forex burden based on international crude oil prices. Energy 2014;73:380–6.
[50] Huang S, An H, Gao X, et al. Identifying the multiscale impacts of crude oil price shocks on the stock market in China at the sector level. Phys A: Stat Mech Its Appl 2015;434:13–24.
[51] Jia X, An H, Fang W, et al. How do correlations of crude oil prices co-move? A grey correlation-based wavelet perspective. Energy Econ 2015;49:588–98.
[52] Jin W, Li Z J, Wei L S, et al. The improvements of BP neural network learning algorithm[C]. In: Signal processing proceedings, 2000. WCCC-ICSP 2000. 5th International conference on IEEE; 2000, 3, p. 1647–9.
[53] Er MJ, Wu S, Lu J, et al. Face recognition with radial basis function (RBF) neural networks. IEEE Trans Neural Networks 2002;13(3):697–710.
[54] Huang GB, Zhu QY, Siew CK. Extreme learning machine: theory and applications. Neurocomputing 2006;70(1):489–501.
[55] Cao J, Zhang K, Luo M, et al. Extreme learning machine and adaptive sparse representation for image classification. Neural Networks 2016;81:91–102.
[56] Diebold FX, Mariano RS. Comparing predictive accuracy. J Bus Econ Stat 2002;20(1):134–44.
[57] Hastie T, Tibshirani R, Friedman J. Neural networks, the elements of statistical learning: data mining, inference, and prediction. New York, NY: Springer New York; 2009. p. 389–416.